Determination of Charge Accumulation and Its Characteristic Time in Double-Barrier Resonant Tunneling Structures Using Steady-State Photoluminescence

Jeff F. Young, B. M. Wood, G. C. Aers, R. L. S. Devine, H. C. Liu, D. Landheer, and M. Buchanan
Division of Physics, National Research Council, Ottawa, Canada K1A0R6

and

A. J. SpringThorpe and P. Mandeville
Bell Northern Research Ltd., Ottawa, Canada K1Y4H7
(Received 19 January 1988)

The steady-state density of electrons accumulated in the well of a GaAs/AlGaAs double-barrier resonant tunneling structure is optically determined as a function of applied voltage by monitoring of the integrated area under the photoluminescence signal from the confined GaAs well. The characteristic time, ≥ 350 ps, obtained as the quotient of the areal charge and current densities, is consistent with calculations of the intrinsic lifetime of the resonant state, independent of intrasubband scattering processes.

PACS numbers: 73.40.Gk, 72.80.Ey, 73.40.Lq

Electron tunneling plays an important role in many branches of physics including tunneling microscopy,[1] tunneling spectroscopy,[2] and resonant tunneling transport,[3] to name but a few. Modern semiconductor growth techniques have made it possible to engineer model tunneling structures with which experiments can be designed to address some of the fundamental aspects of the tunneling process. An outstanding question, which has received much attention for some years, is related to the time scales involved in tunneling processes.[4,5] This point and, more specifically, the question as to the effects of inelastic scattering on this time, have been the subjects of recent debate in the context of electron tunneling through two semiconductor barriers separated by distances on the order of 5 nm.[6-8] In the present work, an optical technique is used to deduce the steady-state occupation of the quasibound two-dimensional level responsible for resonantly enhancing the current through a double-barrier resonant tunneling (DBRT) structure consisting of a GaAs well region sandwiched between AlGaAs barrier layers. The resultant areal charge density in the well is divided by the current density to deduce the voltage dependence of the characteristic time associated with charge accumulation and decay. This experimentally determined time is shown to be consistent with a calculation of the inverse linewidth of the coherent tunneling spectrum appropriate for the structure studied, despite the fact that it is at *least* 350 times longer than the time associated with scattering events in the plane of the layers, $\simeq 1$ ps. This provides evidence that intrasubband scattering does not influence the characteristic tunneling time in DBRT structures.

Experiment.—The sample was grown by molecular-beam epitaxy on a silicon-doped GaAs substrate. The layers' composition is described in Table I. The undoped GaAs is actually *n* type with a residual carrier density of 5×10^{14} cm^{-3} at 4.2 K. In order to probe the GaAs well region optically in the presence of an applied electrical bias, an annular-shaped contact was fabricated on a 325-μm-diam mesa etched through the epilayers. Back contact was made through the substrate. The sample was mounted in an optical cryostat and biased through a 1-Ω series resistor. A 1-mW HeNe laser beam was focused onto the annular contact in order to excite a small population of holes in the well region, buried 1.01 μm below the surface. The light emitted by the device was analyzed in a Spex Triplemate spectrograph, with use of a Si charge-coupled-device array as a detector. All measurements were performed at an ambient temperature of 5 K.

Results.—A plot of the current flowing through the barriers as a function of the voltage across the structure (i.e., the measured potential corrected for the 5.7-Ω contact resistance) is shown in a dotted curve in Fig. 1. Positive bias corresponds to electrons flowing from the top epilayer into the substrate. For applied voltages within the regions of negative differential resistance, the circuit

TABLE I. Layer description.

Layer	Composition	Doping (cm^{-3})	Thickness (nm)	Comments
1	GaAs	2×10^{17}	···	Substrate
2	GaAs	2×10^{18}	500	MBE
3	GaAs	None	7.5	MBE
4	$Al_{0.3}Ga_{0.7}As$	None	10	MBE
5	GaAs	None	5	MBE
6	$Al_{0.3}Ga_{0.7}As$	None	10	MBE
7	GaAs	2×10^{18}	1000	MBE

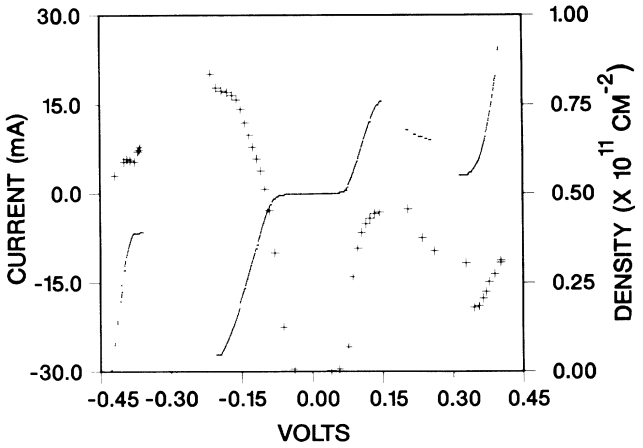

FIG. 1. Dots: The current flowing through the DBRT structure as a function of the voltage across the barriers. Crosses: The ratio of the integrated PL intensity under the peak near 765 nm to that measured with no applied voltage, times the residual electron density in the undoped GaAs well. The voltage scale represents the potential measured across the structure, minus the voltage dropped across the 5.7-Ω series contact resistance.

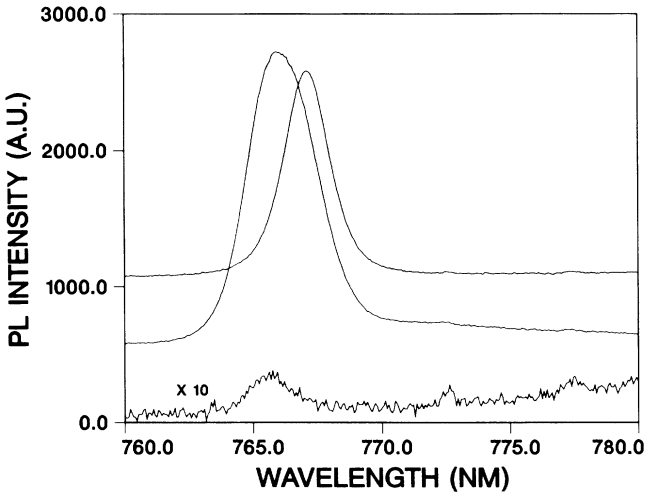

FIG. 2. The PL spectra obtained from the DBRT structure with 0-mV (bottom), 123-mV (middle), and 365-mV (top) applied bias. The base lines of the three spectra are vertically displaced for clarity.

was oscillating. The current and voltages measured with dc voltmeters therefore do not represent the "true" current-voltage (I-V) characteristics of the device for those ranges of applied bias. The asymmetry in the I-V curve reflects the basic asymmetry of the layers in the structure, as it is absent in symmetric structures grown in the same system.

With no current flowing through the structure, the photoluminescence (PL) spectrum consists of a single, 4-meV-wide peak centered at 766 nm, due to transitions involving the first electron and heavy-hole subbands. The intensity of this peak is a factor of $\simeq 10^5$ weaker than the band-edge luminescence from the 1-μm-thick top contact, which is centered around 810 nm. When a bias is applied in the presence of HeNe illumination, dramatic changes in the luminescence from the GaAs well region are observed. Three spectra are shown in Fig. 2, corresponding to bias voltages of 0, 123, and 365 mV. With no HeNe laser radiation incident on the structure, no cathodoluminescence was observed. The dependence of the width and peak position of the luminescence on bias voltage will be discussed elsewhere. Herein, we discuss the bias dependence of the total area under the peak at approximately 765 nm. The area is plotted (crosses) as a function of bias voltage in Fig. 1 (the scale, in units of carrier density, is explained below).

Discussion.—The primary effect of the HeNe illumination is to inject optically a low density of nonequilibrium free holes in the valence band of the GaAs well. The I-V curve is unaffected by the HeNe laser, supporting the fact that a very low density of holes is created. A simple rate-equation analysis for the luminescence output indicates that if the inverse lifetime of the nonequilibrium holes is greater than the radiative recombination rate, which is proportional to the product of the densities of electrons and holes, then the PL output should be proportional to the density of electrons in the well, for a fixed illumination intensity. Time-resolved PL experiments on GaAs quantum well structures[9] suggest that the trapping rate of minority holes on ionized acceptors is larger than the radiative recombination rate for hole concentrations as high as 1×10^{16} cm^{-3}. Thus, at least for low injected electron concentrations, the area under the peak near 765 nm is proportional to the density of electrons in the GaAs well. For large electron densities, a saturation effect is expected as the population of holes is affected by the radiative recombination process. Without independent measurements of the nonradiative hole capture rate and radiative recombination rate for this particular sample, it is difficult to estimate the effective saturation density of electrons. However, given that the area of the PL is significantly larger for negative as opposed to positive bias, the shape of the integrated PL curve, at least for positive bias, does reflect the voltage dependence of the electron density accumulated in the GaAs well. The absolute density scale in Fig. 1 was therefore obtained by scaling of the residual electron density at zero bias, 5×10^{14} cm^{-3} as obtained from Hall measurements, by the integrated PL area normalized with respect to that with no voltage applied to the sample. The other factor which could interfere with the assumed proportionality between integrated PL and electron density is the bias dependence of the oscillator strength associated with the peak in the PL. On the basis of other studies of this phenomenon,[10] for voltages less than 200 mV (fields less than 8×10^4 V/cm) there should only be a small luminescence quenching effect for a 5-nm-thick well.

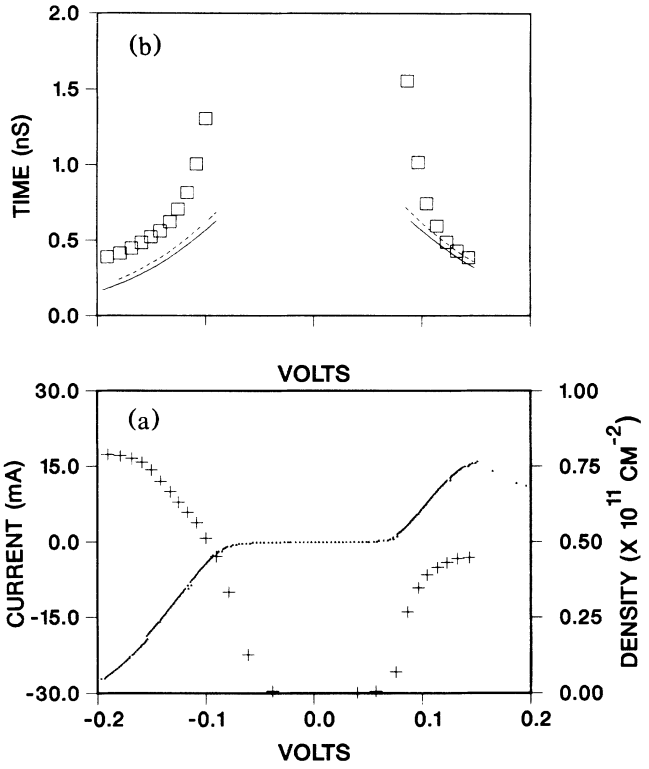

FIG. 3. (a) The same plots of current and accumulated carrier density as in Fig. 1, but on an expanded voltage scale. (b) Squares: The characteristic time obtained as the quotient of the measured areal charge density by the current density at various bias voltages in the resonant tunneling regimes. The dashed curve is a numerical calculation of the characteristic coherent tunneling time, $\tau=\hbar/2\,\mathrm{Im}(E_0)$. The solid curve is the time obtained with use of the approximation for the coherent tunneling time given in Eq. (1).

There is clearly much information contained in the curves of Fig. 1. In this Letter, we confine ourselves to a discussion of the charge and current behavior for applied biases between -200 to -80 mV and 80 to 150 mV: that is for voltages such that the structure is in the resonant tunneling regime, and the circuit is not oscillating. The bottom of Fig. 3 shows the same current- and charge-density plots as in Fig. 1, but on an expanded voltage scale to emphasize the region of interest. The top of Fig. 3 shows a plot of the characteristic time obtained as the quotient of the areal charge density, Q, by the current density, J, at each voltage. If the tunneling process is assumed to be entirely coherent, this time, $\tau=Q/J$, is related to the imaginary part of the quasibound-state eigenenergy, or equivalently, to the half width of the coherent tunneling transmission spectrum,[11] as $\tau=\hbar/2\,\mathrm{Im}(E_0)$. If effective-mass boundary conditions are adopted, an approximate form of this characteristic time can be derived as

$$\tau\sim\frac{2[(m_w/m_b)t+d_e+d_c]}{(2E_R/m_W)^{1/2}(T_e+T_c)}, \tag{1}$$

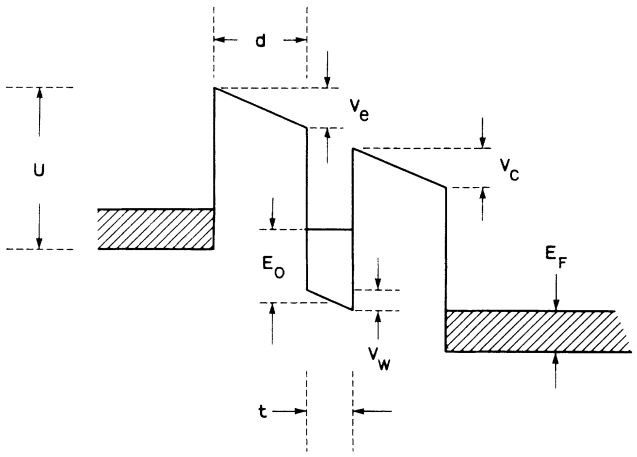

FIG. 4. A schematic representation of the approximate energy-level diagram of the DBRT structure which was adopted for the purpose of calculation.

in the limit that $\mathrm{Im}(E_0)\ll\mathrm{Re}(E_0)$. Here, with reference to Fig. 4, m_w and m_b are the effective masses of the electron in the well and barrier regions, respectively, t is the thickness of the well, $E_R=\mathrm{Re}(E_0)$, T_e and T_c are the transmission coefficients through the emitter and collector barriers, respectively, and d_e and d_c are the effective depths to which the quasibound wave function penetrates into the respective barriers. A WKB calculation of the tunneling process yields the following expressions[12] for $d_{e/c}$ and the $T_{e/c}$:

$$d_{e/c}=\frac{3\hbar eV_{e/c}}{2(2m_b)^{1/2}}[\mp(U-E_R\pm\tfrac{1}{2}eV_w)^{3/2} \pm(U-E_R\pm\tfrac{1}{2}eV_w\pm eV_{e/c})^{3/2}]^{-1} \tag{2}$$

and

$$T_{e/c}=16(E_R/U)(1-E_R/U)\exp(-2d/d_{e/c}). \tag{3}$$

The various energies which appear in Eqs. (2) and (3) are defined in Fig. 4. If the ratio of masses multiplying t in Eq. (1) is neglected (it appears because of the effective-mass boundary conditions), the interpretation of this expression for the characteristic time is clear. The electron, with velocity $v=(2E_R/m_w)^{1/2}$ perpendicular to the layers, moves from just inside one barrier across the well and into the other barrier every $(t+d_e+d_c)/v$ sec. On encountering the ith barrier, it escapes from the well with probability T_i. With $m_w=0.07m_0$, $m_b=0.092m_0$, $U=240$ meV, $t=5$ nm, and $d=10$ nm, a numerical integration of Schrödinger's equation for the structure schematically illustrated in Fig. 4 yields $E_R=74$ meV, and Eq. (1) then gives the approximate characteristic time shown as a solid line in Fig. 3(b). A numerical calculation, based on the "coherent" tunneling picture,[13] of Q/J or $\tau=\hbar/2\,\mathrm{Im}(E_0)$ gives the dashed line in Fig. 3(b). If the T_e term in the denominator of Eq. (1) is omitted to take ac-

count of the fact that when the device is biased in the resonant tunneling regime, the Pauli exclusion principle prevents electrons from tunneling out through the emitter barrier, a result intermediate to the solid and dashed lines in Fig. 3(b) is obtained.

On a qualitative level, a similar decrease of τ with increasing applied voltage is apparent in both experiment and theory. This reflects the increasing probability that the electron can escape through the collector as the applied bias decreases the effective height of the barrier [see Eqs. (2) and (3)]. On a quantitative level there is also quite good agreement between experiment and theory. Given the uncertainty in the material parameters, and that no attempt was made to incorporate self-consistently effects due to charge accumulation or depletion, no better agreement can be expected.

The irrelevance of the lateral scattering rate to the determination of the characteristic tunneling time remains to be explained. In the spirit of the interpretation of Eq. (1) given above, scattering events would be expected to influence the characteristic tunneling time only if they altered either the resonant energy E_R, the transmission coefficient T_c, or both. By definition, intrasubband transitions, that is those which contribute to the mobility of a two-dimensional gas *parallel* to the layers, do not change E_R and thus could only affect τ if there is a significant dependence of T_c on the parallel wave vector of the electron. Our calculations indicate a negligible dependence of T_c on parallel wave vector, even up to values corresponding to room temperature.

Photoluminescence has been used to determine the steady-state carrier density accumulated in a biased DBRT structure. By dividing the areal charge and current densities, we obtained a characteristic tunneling time which is consistent with calculations of the inverse half width of the coherent tunneling spectrum for the sample. This time, ≥ 350 ps depending on the applied bias, is much longer than the characteristic time for intrasubband scattering parallel to the layers. Lateral scattering does not affect the characteristic tunneling time because the perpendicular velocity of the quasi-bound electrons is unaffected by in-plane scattering events.

We would like to acknowledge gratefully the strong support of B. Kettles and R. Boulet throughout this work.

[1]G. Binnig, H. Rohrer, Ch. Gerber, and E. Weibel, Appl. Phys. Lett. **40**, 178 (1982), and Phys. Rev. Lett. **49**, 57 (1982), and **50**, 120 (1983), and Surf. Sci. **131**, L379 (1983).

[2]J. Lambe and R. C. Jaklevic, Phys. Rev. **165**, 821 (1968).

[3]V. J. Goldman, D. C. Tsui, and J. E. Cunningham, Phys. Rev. Lett. **58**, 1256 (1987).

[4]K. W. H. Stevens, J. Phys. C **16**, 3649 (1983).

[5]M. Büttiker and R. Landauer, Phys. Rev. Lett. **49**, 1739 (1982), and Phys. Scr. **32**, 429 (1985), and IBM J. Res. Dev. **30**, 451 (1986), and references therein.

[6]S. Luryi, Appl. Phys. Lett. **47**, 490 (1985).

[7]T. Weil and B. Vinter, Appl. Phys. Lett. **50**, 1281 (1987).

[8]P. J. Price, Phys. Rev. B **36**, 1314 (1987).

[9]J. F. Ryan, R. A. Taylor, A. J. Turberfield, A. Maciel, J. M. Worlock, A. C. Gossard, and W. Wiegmann, Phys. Rev. Lett. **53**, 1841 (1984).

[10]G. Bastard, E. E. Mendez, L. L. Chang, and L. Esaki, Phys. Rev. B **28**, 341 (1983).

[11]P. J. Price, Superlattices Microstruct. **2**, 593 (1986).

[12]V. J. Goldman, D. C. Tsui, and J. E. Cunningham, Phys. Rev. B **35**, 9387 (1987).

[13]R. Tsu and L. Esaki, Appl. Phys. Lett. **22**, 562 (1973).